Comparison of High-degree Solar Acoustic Frequencies and Asymmetry between Velocity and Intensity Data

S. C. Tripathy

National Solar Observatory, Tucson, AZ 85719, USA

stripathy@nso.edu

H. M. Antia

Tata Institute of Fundamental Research, Homi Bhabha Road, Mumbai 400 005, India

K. Jain and F. Hill

National Solar Observatory, Tucson, AZ 85719, USA

ABSTRACT

Using the local helioseismic technique of ring diagram we analyze the frequencies of high–degree *f*- and *p*-modes derived from both velocity and continuum intensity data observed by MDI. Fitting the spectra with asymmetric peak profiles, we find that the asymmetry associated with velocity line profiles is negative for all frequency ranges agreeing with previous observations while the asymmetry of the intensity profiles shows a complex and frequency dependent behavior. We also observe systematic frequency differences between intensity and velocity spectra at the high end of the frequency range, mostly above 4 mHz. We infer that this difference arises from the fitting of the intensity rather than the velocity spectra. We also show that the frequency differences between intensity and velocity do not vary significantly from the disk center to the limb when the spectra are fitted with the asymmetric profile and conclude that only a part of the background is correlated with the intensity oscillations.

Subject headings: Sun: helioseismology –Sun: oscillations – Sun: interior

1. Introduction

Different helioseismic instruments, both from ground and space, observe the Sun in different observables. Due to the different techniques used by these instruments, it is possible

to measure the solar oscillations simultaneously either as variations in the photospheric velocity or as intensity fluctuations. It is therefore important to confirm that the oscillation mode parameters measured from both the intensity and velocity agree with each other to a high degree of precision. However, the initial measurement of low degree p-mode frequencies from Doppler velocity (V) and continuum intensity ($\mathrm{I_c}$) observations from Michelson Doppler Imager (MDI) instrument on board *Solar and Heliospheric Observatory* (SOHO) showed systematic differences. A comparison of 108-day power spectra between V and $\mathrm{I_c}$ showed a weighted mean difference of -0.1 μHz for $\ell = 0$, and -0.16 μHz for $\ell = 1$ modes (Toutain et al. 1997). Since the apparent frequency shift between an oscillation observed in velocity and intensity cannot be a property of the mode, it must arise from systematic errors while calculating the frequencies from the observed power spectra. Hence it was argued that the source of the systematic difference could be due to the opposite asymmetry effect seen between the velocity and intensity power spectra (Duvall et al. 1993). Appourchaux et al. (1998) also presented a similar evidence using VIRGO and SOI/MDI data. Around the same time Harvey et al. (1998) reported that the intermediate degree modes observed in V and total spectral intensity also show different central frequencies and observed that the apparent differences could be as large as 50 μHz close to the acoustic cut-off frequency. However, the analysis of Nigam & Kosovichev (1998), using an asymmetric line profile-fitting formula, illustrated that the frequency difference between V and $\mathrm{I_c}$ in the intermediate degree range is much smaller compared to that obtained by fitting a symmetric Lorentzian profile. Using the same asymmetric line profile-fitting formula, Toutain et al. (1998) re-analyzed the data from MDI and showed that the frequency differences between V and $\mathrm{I_c}$ are considerably reduced. Gavryusev & Gavryuseva (1999) have also analyzed data from different instruments and have argued that the reported frequency shift is merely an artifact of the reduction technique.

Renewed interest in the topic began when local helioseismic techniques were developed to study the properties of high-degree modes in localized regions. Basu, Antia, & Bogart (2001) analyzed azimuthally averaged (2-d) power spectra and inferred that the eigenfrequencies obtained using the asymmetric peak profiles agree reasonably well with each other while the use of symmetric profiles gives significant differences between frequencies computed using continuum intensity and velocity or continuum intensity and line-depth spectra. In order to gain further information for high-degree and high-frequency modes, Jain, Hill, & Toner (2003) analyzed the high-resolution GONG+ data. These authors also compared the azimuthally averaged power spectra of a region centered on the equator and reported that the frequency dependence of the frequency shift between V and I is negligible below the acoustic cutoff frequency around 5.3 mHz and substantial above the cutoff. These results supported the finding of Harvey et al. (1998). However, the conclusion is based on the visual comparison of the peak frequency of the power spectra and may not necessarily be

a true measure of the shift due to the reversal of the asymmetry and different background power between V and I_c spectra.

It is now well established that line asymmetry of the solar power spectra alters the peak frequencies that are obtained under the assumption that the lines are symmetric (e.g. Antia & Basu (1999); Basu & Antia (2000). However, the cause of the opposite asymmetry between the velocity and intensity spectra still remains inconclusive. The current understanding is that the reversal in the sign of asymmetry between the V and I_c spectra is due to the influence of the solar background noise that is correlated with the source (Roxburgh & Vorontsov 1997; Nigam et al. 1998; Severino et al. 2001) and the level depends on the characteristic granulation. On the other hand, the numerical simulation (Georgobiani, Stein, & Nordlund 2003) indicates that the reversal is produced by the radiative transfer effects. Since the physics of the correlated noise is not yet fully understood and the spatial leakage signature for V and I is different due to their center-to-limb variations, our objective is to examine the frequency dependence of the observed asymmetry and differences in eigenfrequencies between velocity and intensity observations as a function of the radial distance from the disk center to the limb. A preliminary investigation of a similar nature using azimuthally averaged power spectra is reported in Tripathy et al. (2006). However the present analysis differs from all earlier ones since here we use the three-dimensional (3-d) power spectrum, which is associated with flow fields, while the azimuthally averaged spectrum has no flow fields associated with it.

The rest of the paper is organized as follows: We briefly describe the data and analysis technique in Section 2, while the results are described in Section 3. Finally, we summarize the main conclusions in Section 4.

2. Data and the Technique

We use the Dopplergrams and continuum intensity images obtained by the MDI instrument during the period of 1997 May 19 – 21 when solar activity was near minimum. We have chosen 4 regions centered at heliographic longitudes of 0°, 15°, 30°, and 45°; all centered at the equator. The spatial extent of each of the localized region covers 256×256 pixels in heliographic longitude and latitude and gives a resolution of 0.01616 Mm^{-1}. Each region is tracked for 4096 minutes, which gives a frequency resolution of 4.07 μHz. The standard ring diagram technique (Hill 1988) was used to obtain the power as a function of (k_x, k_y, ν).

To extract the frequencies and other mode parameters, the three-dimensional power

spectrum is fitted with a model with asymmetric peak profiles of the form

$$P(k_x, k_y, \nu) = \frac{e^{B_1}}{k^3} + \frac{e^{B_2}}{k^4} + \frac{exp(A_0 + (k-k_0)A_1 + A_2(\frac{k_x}{k})^2 + A_3\frac{k_x k_y}{k^2})S_x}{x^2+1} \quad (1)$$

where

$$x = \frac{\nu - ck^p - U_x k_x - U_y k_y}{w_0 + w_1(k-k_0)}, \quad (2)$$

$$S_x = S^2 + (1+Sx)^2. \quad (3)$$

Here P is the oscillation power for a mode with a temporal frequency ν and the total wavenumber $k = \sqrt{k_x^2 + k_y^2}$. The peak power in the mode is represented as $\exp(A_0)$ while the coefficients A_1 to A_3 account for the variation in power with k and along the ring. The terms involving B_1 and B_2 define the background power and w_0 is the mode width. The term ck^p gives the mean frequency, and this form is chosen as it gives satisfactory fits to the mean frequency over the whole fitting interval. The parameters S controls the asymmetry in the peaks, and the form of asymmetry is the same as that used by Nigam & Kosovichev (1998) i.e. the parameter is positive for positive asymmetry and negative for negative asymmetry. By setting $S = 0$ we can also fit symmetric Lorentzian profiles. A more detailed description of the parameters and fitting procedure is described in Basu, Antia, & Tripathy (1999) and Basu & Antia (1999). The 13 parameters (A_0, A_1, A_2, A_3, B_1, B_2, c, p, S, U_x, U_y, w_0, w_1) are determined by fitting the spectra using the maximum likelihood approach (Anderson, Duvall, & Jefferies 1990). In this work we express k in units of $R_\odot^{-1}$ so that k is identified with the degree ℓ of the spherical harmonic of the corresponding global mode.

3. Results and Discussions

Figure 1 shows a characteristic $\ell - \nu$ diagram obtained from the fits to the power spectra at the disk center using asymmetric profile corresponding to Eq. (1). In general we obtain about 750 and 600 modes from the velocity and intensity spectra respectively. Intensity spectra normally yields less number of modes due to the inherently lower signal-to-noise ratio. The number of fitted modes also decreases for regions that are away from the disk center. Comparing the number of modes between symmetric and asymmetric fits we find that the symmetric fit yields more modes. This implies that the inclusion of the asymmetry in the fitting formula reduces the number of modes that are successfully fitted. This could be due to some cross-correlation between S and other parameters of the model, particularly,

the background. Although, we fit the spectra up to radial order of $n = 6$, we restrict the analysis up to $n = 4$ modes since higher order radial modes have large estimated fitting errors.

3.1. Asymmetry of Peak Profiles

Physically, asymmetry is a result of an interaction between an outward-directed wave from the source and a corresponding inward-directed wave that passes through the region of wave propagation (Duvall et al. 1993). To illustrate the peaks in the power spectra and to visualize the asymmetry associated with different observables, we show an example of the azimuthally averaged power for $\ell = 675$ corresponding to the disk center spectra for V and $\mathrm{I_c}$ in Figure 2. It is apparent that the line profiles are asymmetric. At low frequency, the asymmetry agrees with the known results; the velocity spectrum has negative asymmetry i.e. more power on the lower frequency side of the peak while the continuum intensity spectrum show positive asymmetry i.e. more power on the higher frequency side of the peak. This reversal of asymmetry is believed to arise from the addition of correlated noise to the amplitude spectra (Nigam et al. 1998). In addition, we notice that the asymmetry associated with velocity spectra appears to be reduced or even reversed at higher frequencies. Visual inspection of the azimuthally averaged power spectra show a comprehensible frequency shift of the central frequency between V and $\mathrm{I_c}$ above the cutoff frequency of 5.3 mHz. We also observe that the velocity power is higher near the disk center and decreases toward the limb in agreement with the predominately radial nature of the oscillatory velocity field.

Figure 3 shows the asymmetry of the line profiles as a function of frequency obtained from fitting the three dimensional power spectra at disk center and 45° E longitude. As expected, this parameter is predominantly negative for all modes in the velocity spectra (upper panels) indicating that there is more power on the low frequency side of the peak. The asymmetry is minimum around 3 mHz while at low end of the frequency range the asymmetry of p_2 and higher order radial modes is more likely to be zero within the estimated errors. Thus, in this frequency range the mode frequencies obtained from asymmetric and symmetric profiles should be nearly identical. Surprisingly, we do not observe the asymmetry to be reversed at higher frequencies as noted above and also in Tripathy et al. (2006).

The asymmetry for the intensity spectra (lower panels of Figure 3) appears to be more complex and in general these are larger than the velocity asymmetry. For f and p_1-modes, this parameter is primarily positive (more power on the higher frequency end of the peak) and increases with frequency. For higher order p-modes, asymmetry is negative both at low- and high-end of the frequency range and is likely to be insignificant or zero at other

frequencies. Thus the asymmetry is different than what is observed for low-degree modes (Toutain et al. 1998), intermediate degree modes (Nigam et al. 1998), and high-degree modes obtained from the azimuthally averaged spectra (Tripathy et al. 2006). Although most of these differences may be due to frequency, we do not rule out the possibility that the form of asymmetry used in the model are simplified and may not represent the real profiles adequately at all frequencies. The asymmetry may also weakly depend on ℓ (Basu & Antia 1999) and this dependence has been neglected in the fitting formula. Finally, we note that the asymmetry of both velocity and intensity spectra do not show any significant changes at different locations on the solar disk.

3.2. Comparison of asymmetry between 2-d and 3-d fitting

It is interesting to compare the asymmetries from 3-d spectra with those obtained from azimuthally averaged spectra. Figure 4 illustrates the asymmetries obtained from both the fits. While the asymmetry observed in intensity spectra obtained from 2-d fits are entirely positive, the behavior is more complex in the 3-d spectra. On the other hand, asymmetry associated with 3-d velocity spectra is entirely negative while for 2-d spectra, it reverses sign at high end of the frequency range. Thus significant differences are seen between the asymmetry obtained from fitting the three-dimensional and azimuthally averaged power spectra.

Although it is not easy to understand these differences due to the different functional form of the model profiles to fit different spectra (six parameters are fitted in azimuthal spectra as opposed to 13 in the three-dimensional spectra), we have made a preliminary attempt by constructing synthetic 3D spectra with $S = -0.05$. This spectra are then azimuthally averaged and fitted to calculate the asymmetry in peak profiles. Because of non-zero values of velocities (U_x, U_y) the process of azimuthal averaging also introduces some asymmetry and hence the value of S in azimuthally averaged spectra is not the same as that used in preparing the 3D spectra. The effect of varying the flow velocity (U_x & U_y) and background term, B_1 is shown in Fig 5. The synthetic spectra were constructed with a uniform amplitude $A_0 = 50$, width $w_0 = 40$ μHz and included only the f-mode ridge. The background in synthetic spectra included only the first term with different values of B_1. The effect of velocity increases with k and hence the shift in asymmetry from input value also increases with k. Further, since A_0 and B_1 are constant, the peak to background ratio increases with k. It is clear that even when the flow velocities are increased beyond their normal values, the maximum change in S is about than 0.02 at the highest value of ℓ and rather large velocity is required to make significant differences. Similar results are obtained

when spectra with different values of S were used. In all cases azimuthal averaging tends to increase the value of S, though the effect may be small.

3.3. Source of the asymmetry

Peak asymmetry is believed to have a contribution from the acoustic source location and a contribution from the effects of correlated background noise from the source. Roxburgh & Vorontsov (1997) have argued that the line asymmetries occur due to the modes correlated with velocity background while to reach the same effect, Nigam et al. (1998) have proposed a small amount of intensity-correlated background. The amount of coherent correlated background, as well as the need of this component to model both V and $\mathrm{I_c}$, has also been debated (e.g. Straus et al. (2001)).

In order to understand the role of the background power in the reversal of the asymmetry between V and $\mathrm{I_c}$, we plot the background power as a function of degree ℓ of the mode in Figure 6. In the same plot, we also show the background power obtained from the symmetric fits (open symbols). It is clear that the background power obtained from symmetric and asymmetric fitting of the velocity spectra (upper panel) closely agree with each other. In contrast the intensity spectrum returns a significantly higher background power when fitted with the asymmetric line profile compared to the symmetric profile. This indicates that the line asymmetry is reversed in the intensity. Since granulation contrast decreases from the disk center to the limb, we also expect the background power to decrease near the limb. But no significant variation in power is noticed from the disk center to the limb which supports the idea that only a part of the background is correlated with the intensity oscillations (Nigam & Kosovichev 1999; Barban & Hill 2004).

3.4. Frequency Differences

The frequency differences from the symmetric fits to both V and $\mathrm{I_c}$ spectra at four different longitudes are plotted in Figure 7. The frequencies obtained from the intensity spectrum are systematically higher than the frequencies from the velocity spectrum, as one would expect due to the reversal of the line asymmetry. For the disk center spectra, the differences, in general, are on the order of 10 μHz or less up to $\nu \leq 4$ mHz; the minimum difference of about 2–3 μHz is seen for p_2 and higher radial order modes in the 5–min band. Since near the limb we primarily observe the horizontal velocity field which is dominated by granulation, it is expected that the frequency difference between intensity and velocity should

decrease near the limb due to a decrease in correlation with oscillations. But we find that the difference increases systematically from the disk center to the limb. This again supports the idea that only a part of the background is correlated with the intensity oscillations.

The use of asymmetric profiles to fit the power spectra results in a better determination of the mode frequencies and as a result the frequency differences between velocity and intensity is significantly diminished (Figure 8). Similar to fits with symmetric profiles, the differences are mostly positive as the frequencies obtained from intensity fluctuations are higher than those from the velocity. However, the *f*-modes show some exception at the high end of the frequency where the peak frequencies observed in velocity are marginally higher (and clearly larger than the estimated errors) than those observed in intensity. The differences between higher order radial modes, mainly p_3 and p_4, are slightly bigger but these modes also have a large uncertainty in the fitted frequencies as seen from the error estimates. Although subtle variations are evident between different longitudes, the frequency differences do not reveal any systematic trend between the disk center and 45° longitude.

Although the asymmetric fitting formula reduces the frequency differences between the velocity and intensity spectra, there still remains some systematic differences of the order of $5-10$ μHz, which is much higher than the uncertainty in estimated errors. Basu, Antia, & Bogart (2001) have reported a similar result based on the analysis of azimuthally averaged spectra and have argued that the assumed profiles does not adequately describe the velocity spectra where the signal-to-noise ratio is high. However, our result indicates that the form of asymmetry used for intensity spectra may not be a correct representation of the real profiles. To demonstrate this, we show the difference in eigenfrequencies between identical modes obtained from the power spectra at different longitudes with respect to the spectra at the disk center in Figure 9. The frequency difference in V shows little variation in longitude for frequencies less than 3.5 mHz. Variations between intensity spectra are higher than seen in velocity. Moreover, the shapes of the curve in Figure 9 for velocity are similar as are the shapes of the curves in intensity, leading to the frequency differences shown in Figure 8. Therefore it appears that the use of an asymmetric line profile provides more accurate estimates of the eigenfrequencies of solar oscillation for velocity rather than for intensity. In addition, fitting the intensity spectra is more challenging than fitting the velocity spectra due to low amplitudes and low signal-to-noise ratio. The number of modes fitted from the intensity spectra clearly supports this conjecture.

4. Conclusions

Using the local helioseismic technique of ring diagram analysis we have studied the high-degree *f*- and *p*-mode frequency differences between velocity and continuum intensity data obtained from the MDI instrument during a quiet period. Since the spectra are known to be asymmetric, we fitted the three-dimensional spectra with an asymmetric model profile based on the known form of the asymmetry observed in velocity and intensity. The asymmetry obtained from fitting the velocity spectra agrees with the previous results while that of intensity shows a frequency dependent behavior. We further notice significant differences between the asymmetry obtained from fitting the three-dimensional and azimuthally averaged power spectra.

Fitting the three-dimensional disk center power spectra with a symmetric Lorentzian profiles leads to frequency differences on the order of 10 μHz or less up to $\nu \leq 4$ mHz between intensity and velocity. This difference is found to be increasing systematically from the disk center to the limb. The use of asymmetric profiles leads to frequency differences that are smaller than the differences resulting from the symmetric fits. However, systematic differences still remain at the high end of the frequency range, mostly above 4 mHz. We demonstrate that this difference arises from the fitting of the intensity rather than the velocity spectra. We speculate that the form of asymmetry used in the model for the intensity spectra is over-simplified and does not adequately represent the real profile at all frequency ranges.

We also conclude that the frequency differences between velocity and intensity do not vary significantly from the disk center to the limb. However, variations between intensity spectra are higher than seen in velocity. This supports the idea that only a part of the background is correlated with the intensity oscillations. In this context several authors (e.g. Severino et al. (2001); Barban, Hill & Kras (2004); Toutain et al. (2006)) have advocated the importance of fitting the intensity-velocity cross spectrum along with a multicomponent model of the coherent background. This provides an impetus for future work using the high-resolution observations from *Solar Dynamics Observatory*.

This study uses data from MDI/SOHO. SOHO is a mission of international cooperation between ESA and NASA. This work was supported by NASA grant NNG 5-11703 and NNG 05HAL41I.

REFERENCES

Anderson, E., Duvall, T. L., Jr., & Jefferies, S. 1990, ApJ, 364, 699

Appourchaux, T., Andersen, B., Chaplin, W. et al. 1998, in Structure and Dynamics of the Interior of the Sun and Sun-like Stars, eds. S. Korzennik & A. Wilson, (ESA-SP 418; Noordwijk: ESA), 95

Antia, H. M. & Basu, S. 1999, ApJ, 519, 400

Barban, C. & Hill, F. 2004, Sol. Phys., 220, 399

Barban, C., Hill, F., & Kras, S. 2004, ApJ, 602, 516

Basu, S., & Antia, H. M. 1999a, ApJ, 525, 517

Basu, S., & Antia, H. M. 2000, ApJ, 531, 1088

Basu, S., Antia, H. M., & Bogart, R. S. 2001, in Helio- and Asteroseismology at the Dawn of the Millennium, ed. A. Wilson (ESA-SP 464; Noordwijk: ESA), 183

Basu, S., Antia, H. M., & Tripathy, S. C. 1999, ApJ, 512, 458

Duvall, T. L., Jr., Jefferies, S. M., Harvey, J. W., Osaki, Y., & Pomerantz, M. A. 1993, ApJ, 410, 829

Gavryusev, V. V., & Gavryuseva, E. A. 1999, Sol. Phys., 189, 261

Georgobiani, D., Stein, R. F., & Nordlund, A. 2003, ApJ, 596, 698

Haber, D., Hindman, B. W., Toomre, J., Bogart, R. S., Larsen, R. M., & Hill, F. 2002, ApJ, 570, 885

Hill, F. 1988, ApJ, 333, 996

Harvey, J. W., Hill, F., Komm, R. W., Leibacher, J., Pohl, B., & the GONG 1998, in New Eyes to See Inside the Sun and Stars, eds. F.-L. Deubner, J. Christensen-Dalsgaard, & D. Kurtz, (IAU publication, The Netherlands), 49

Jain, K., Hill, F., & Toner, C. 2003, in Probing the Sun with High Resolution, eds. S. C. Tripathy & P. Venkatakrishnan, (Narosa Publishing House, New Delhi), 31

Kumar, P. & Basu, S. 1999, ApJ, 519, 396

Nigam, R., & Kosovichev, A. G. 1998, ApJ, 505, L51

Nigam, R., Kosovichev, A. G., Scherrer, P. H., & Schou, J. 1998, ApJ, 495, L115

Nigam, R., & Kosovichev, A. G. 1999, ApJ, 514, L53

Roxburgh, I. W. & Vorontsov, S. V., 1997, MNRAS, 292, L33

Severeno, G., Magri, M., Oliviero, M., Straus, Th ., & Jefferies, S. M. 2001, ApJ, 561, 444

Straus, Th., Severeno, G., Magri, M., & Oliviero, M. 2001, in Helio- and Asteroseismology at the Dawn of the Millennium, ed. A. Wilson (ESA-SP 464; Noordwijk: ESA), 607

Tripathy, S. C., Jain, K., Hill, F., & Toner, C. 2003, Bull. Astr. Soc. India, 31, 321

Tripathy, S. C., Antia, H. M., Hill, F., Jain, K., & González Hernández, I. 2006, in Beyond the Spherical Sun, ed. K. Fletcher, (ESA-SP 624; Noordwijk: ESA), 104

Toutain, T. et al. 1997, Sol. Phys., 175, 311

Toutain, T., Appourchaux, T., Frohlich, C., Kosovichev, A. G., Niram, R., & Scherrer, P. H. 1998, ApJ, 506, L147

Toutain, T., Elsworth, Y., & Chaplin, W. J. 2006, MNRAS, 371, 1731

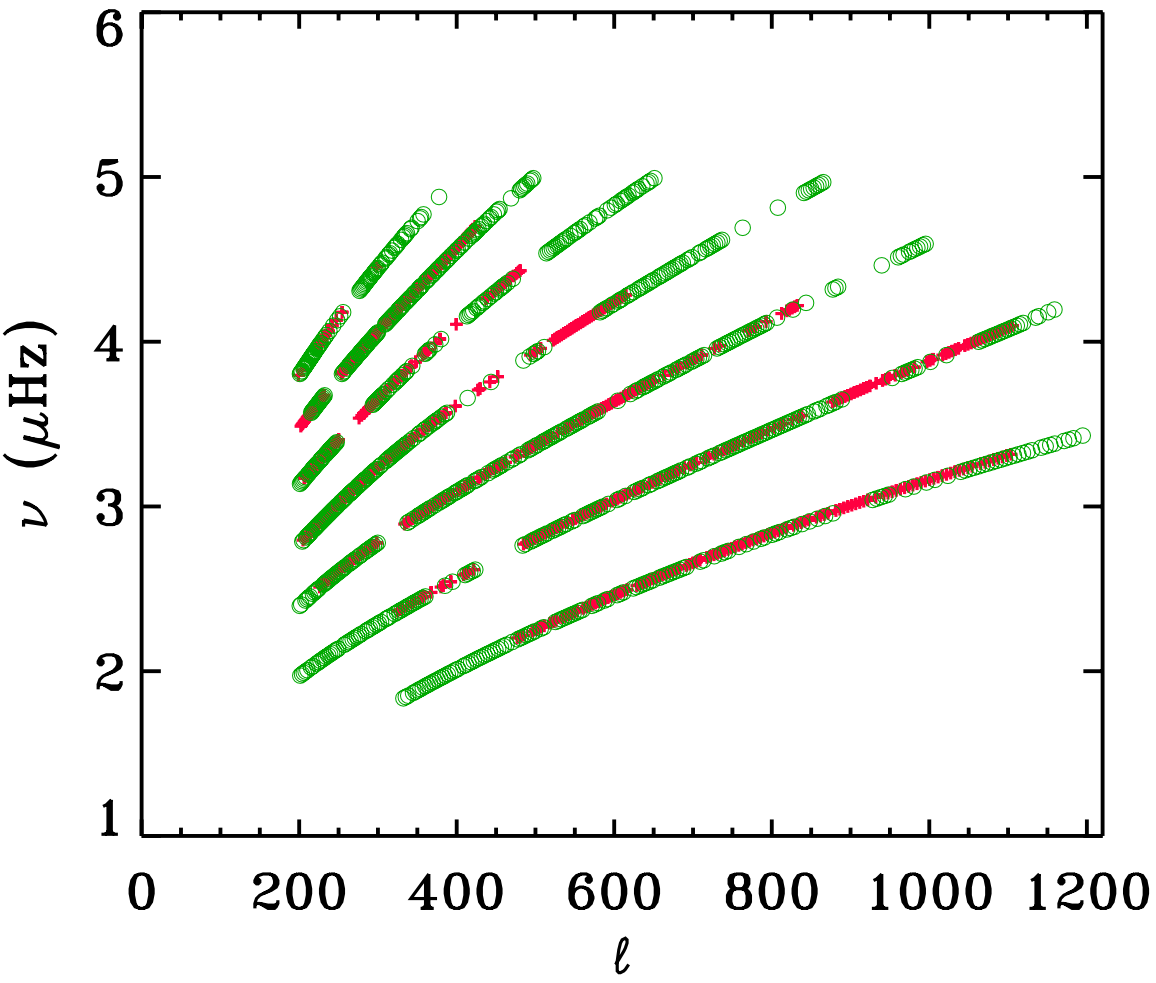

Fig. 1.— The $\ell - \nu$ diagram constructed from the asymmetric fits to disk center spectra for velocity (circles) and continuum intensity (pluses).

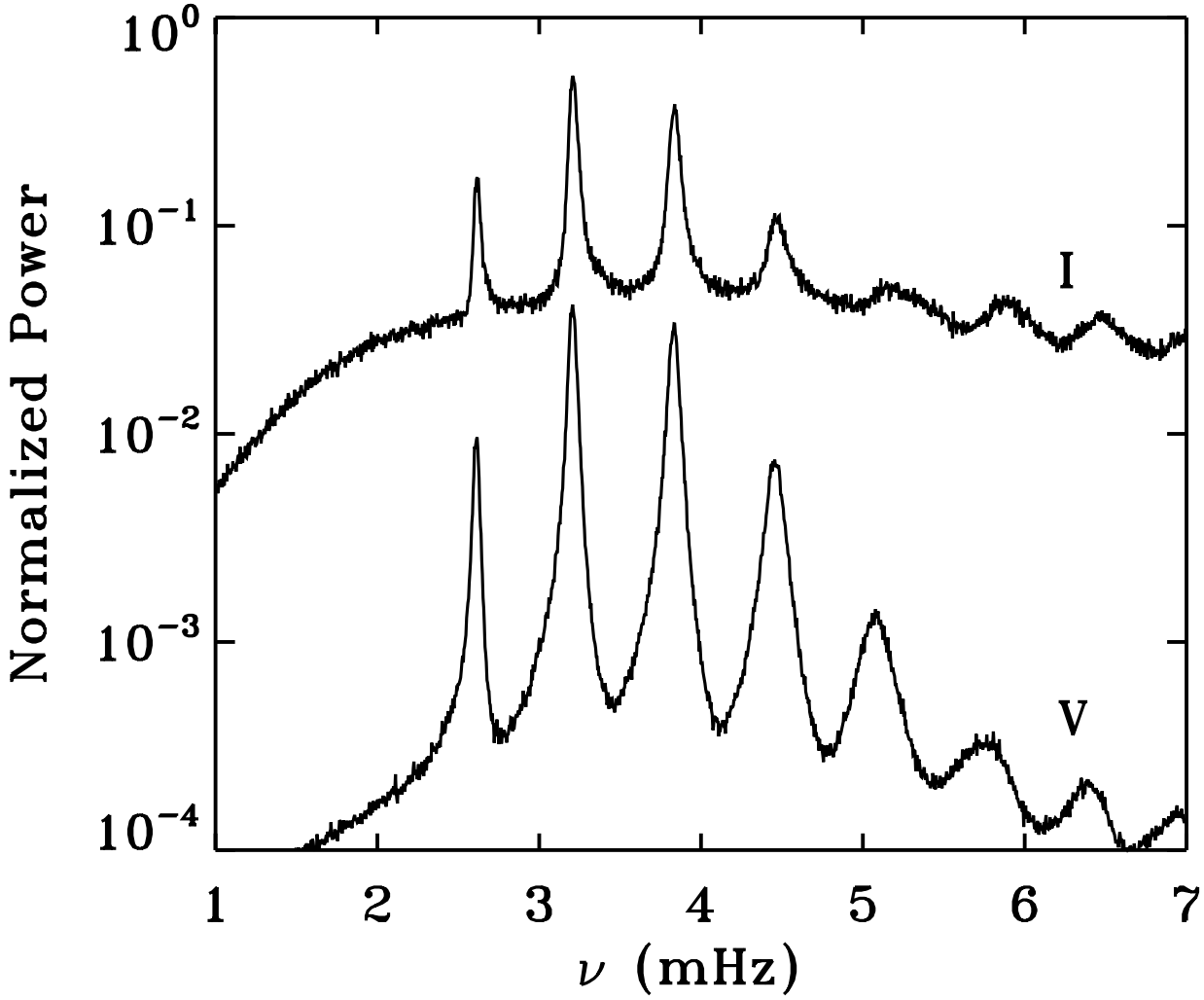

Fig. 2.— Normalized power for $\ell = 675$ corresponding to the azimuthally averaged and normalized velocity and continuum intensity disk center power spectra.

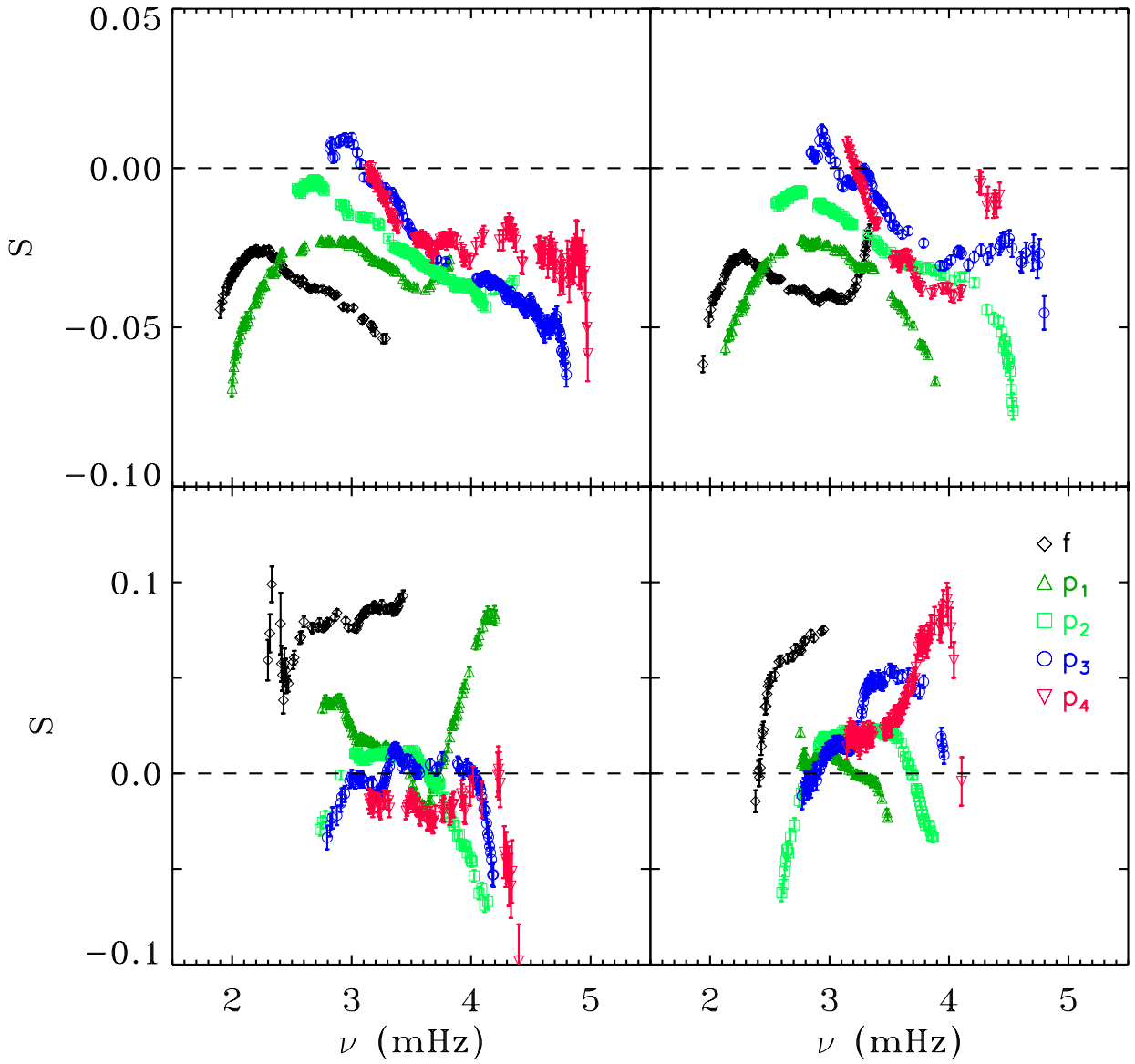

Fig. 3.— Asymmetry parameter S obtained from fits to velocity (top panel) and continuum intensity (bottom panel) spectra at two different locations. The left and right panels refer to the regions at disk center and at a longitude of 45° E, respectively. The symbols represent different radial orders and are explained in the right bottom panel.

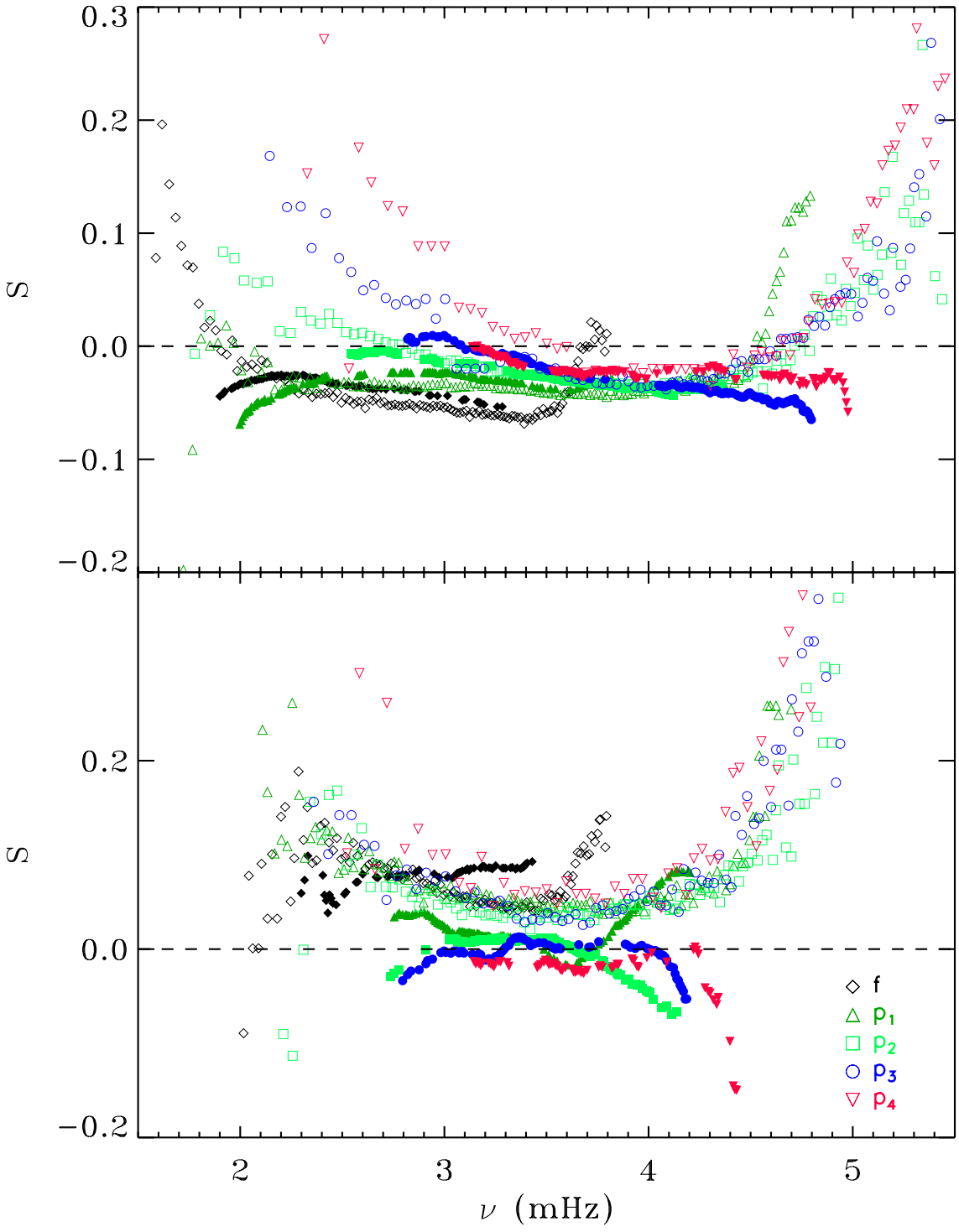

Fig. 4.— Comparison of the asymmetry parameter obtained from fits to three-dimensional (filled symbols) and azimuthally averaged spectra (open symbols) at disk center. The top panel is for velocity and bottom panel is for continuum intensity. The errors are not shown for clarity.

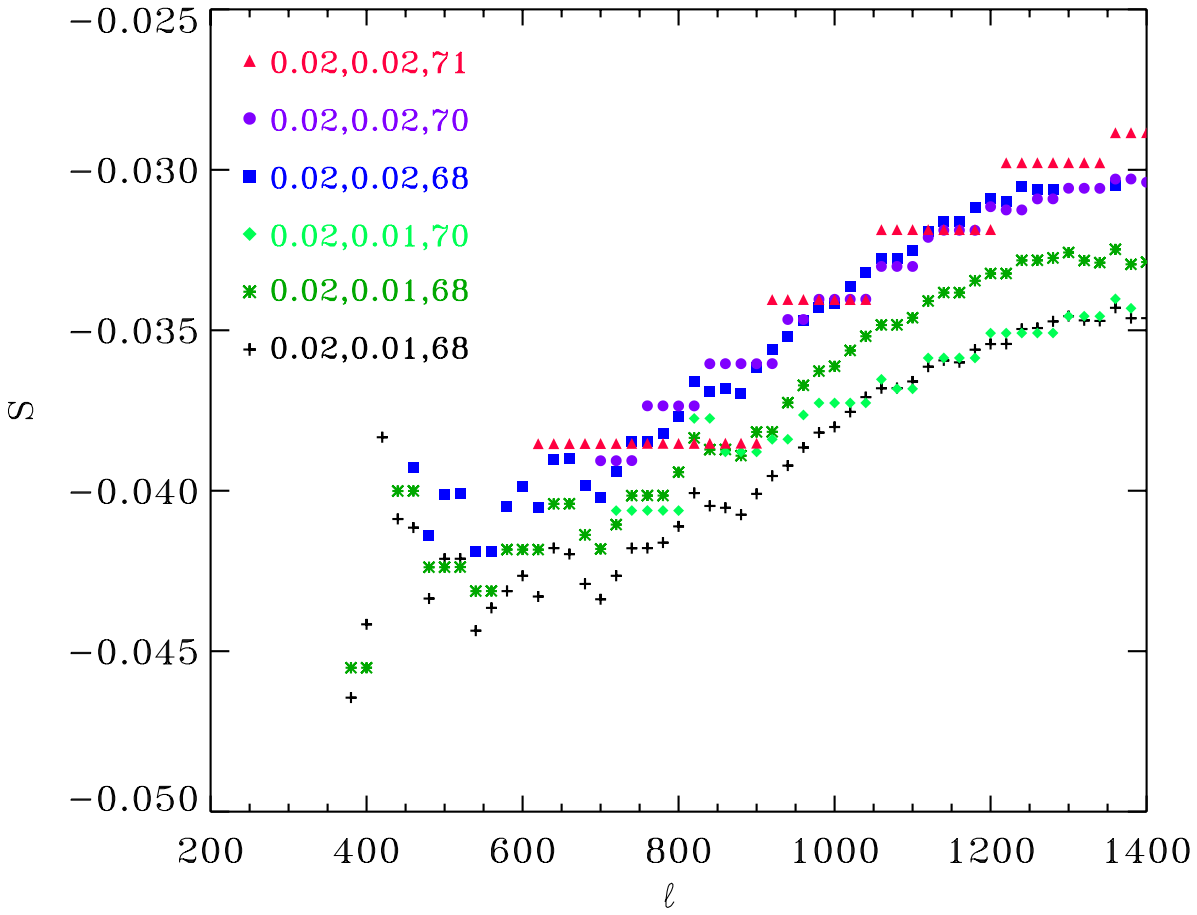

Fig. 5.— The variation in the asymmetry parameter as a function of the flow velocity and background and is obtained from the fitting of azimuthally averaged synthetic spectra. The three values mentioned against each of the symbols represent U_x, U_y and B_1 component, respectively. A value of 0.01 for U_x and U_y corresponds to actual velocity of 43.72 m/s.

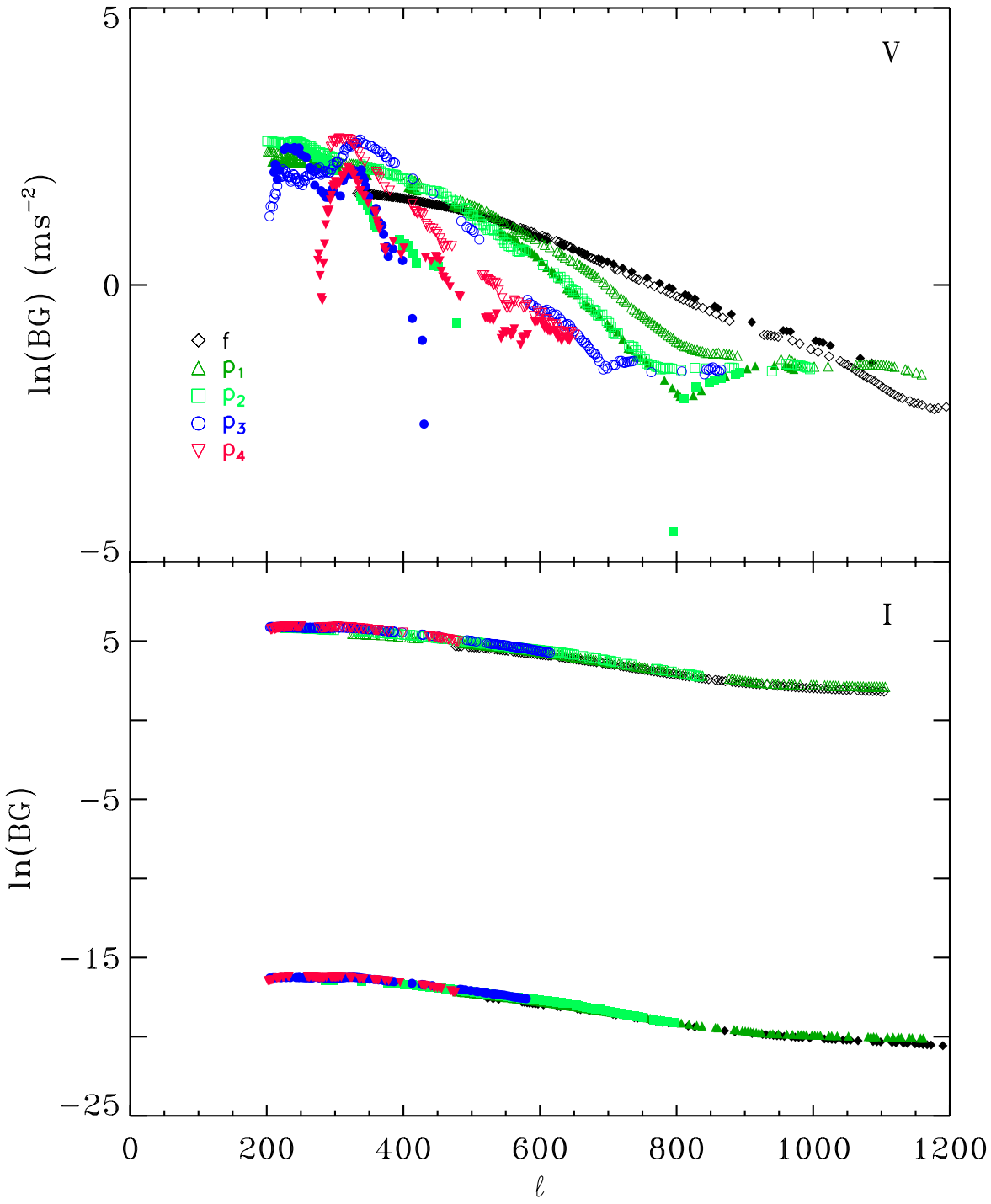

Fig. 6.— Comparison of the background power obtained from symmetric (filled symbols) and asymmetric (open symbols) fits to the disk center spectra. The upper panel is for velocity and bottom panel is for continuum intensity.

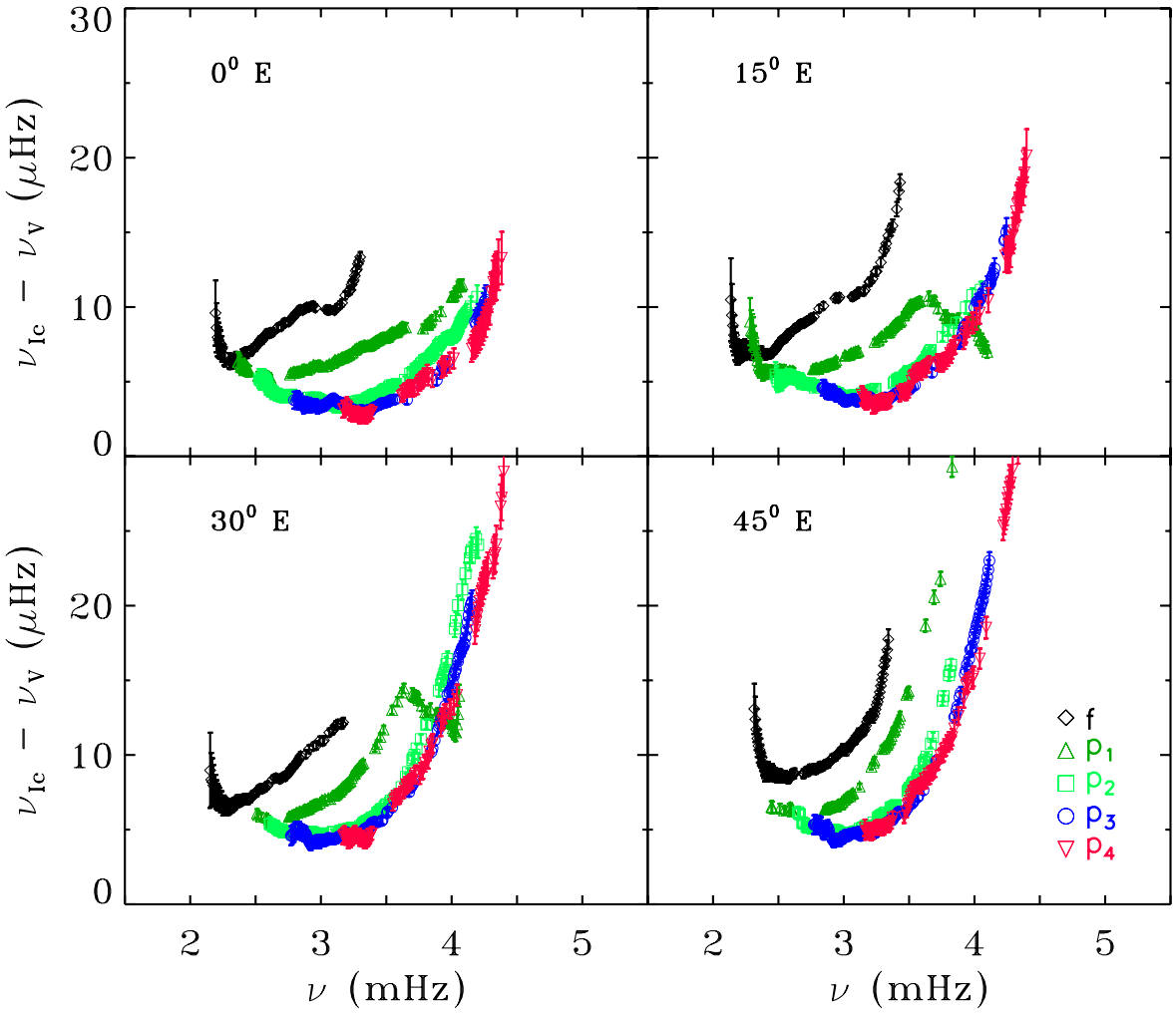

Fig. 7.— Frequency shifts between velocity and continuum intensity modes fitted using symmetric profile at four different longitudes. The locations are marked in each panel.

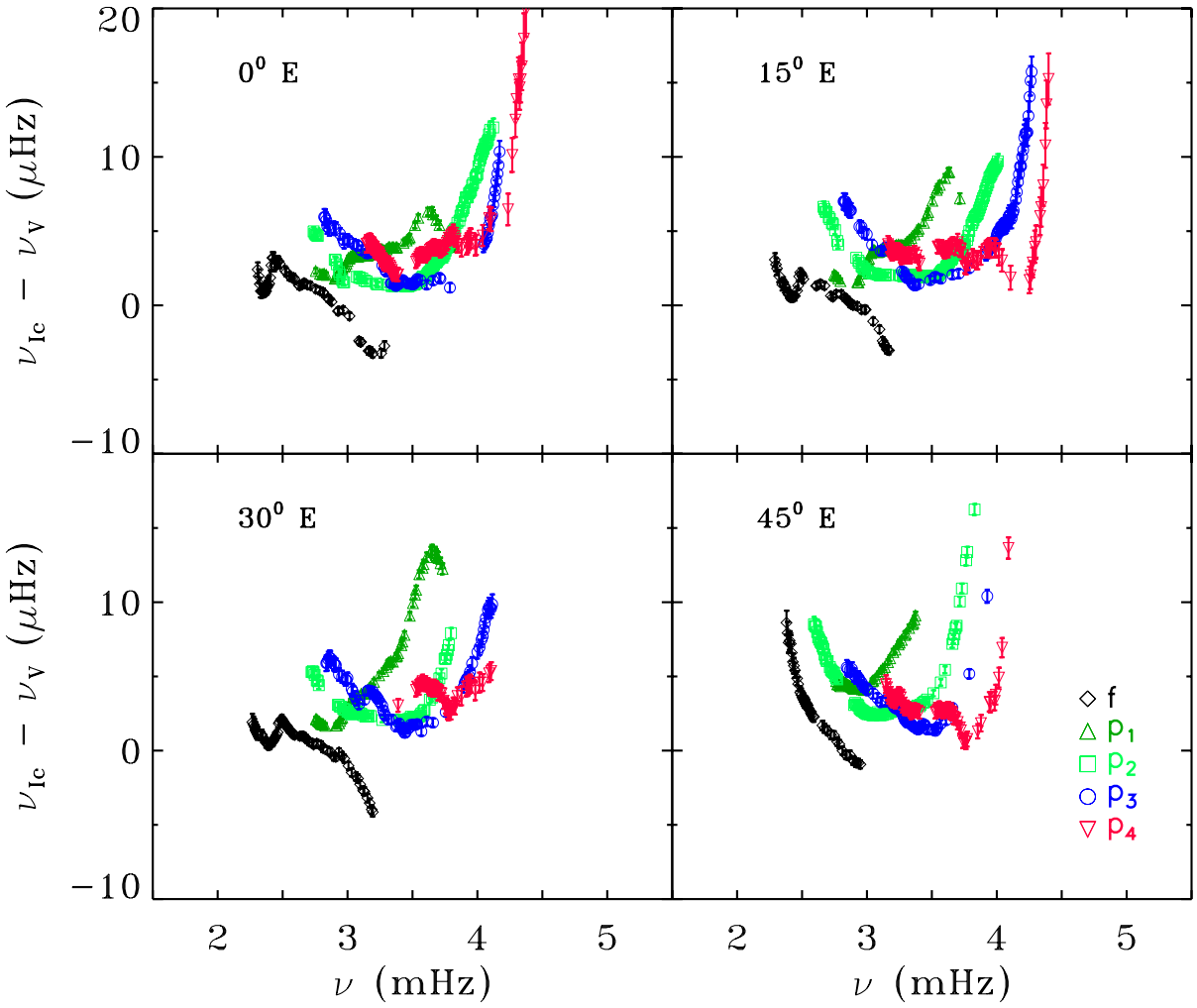

Fig. 8.— Same as Figure 7 but for modes obtained from the fit using asymmetric profiles.

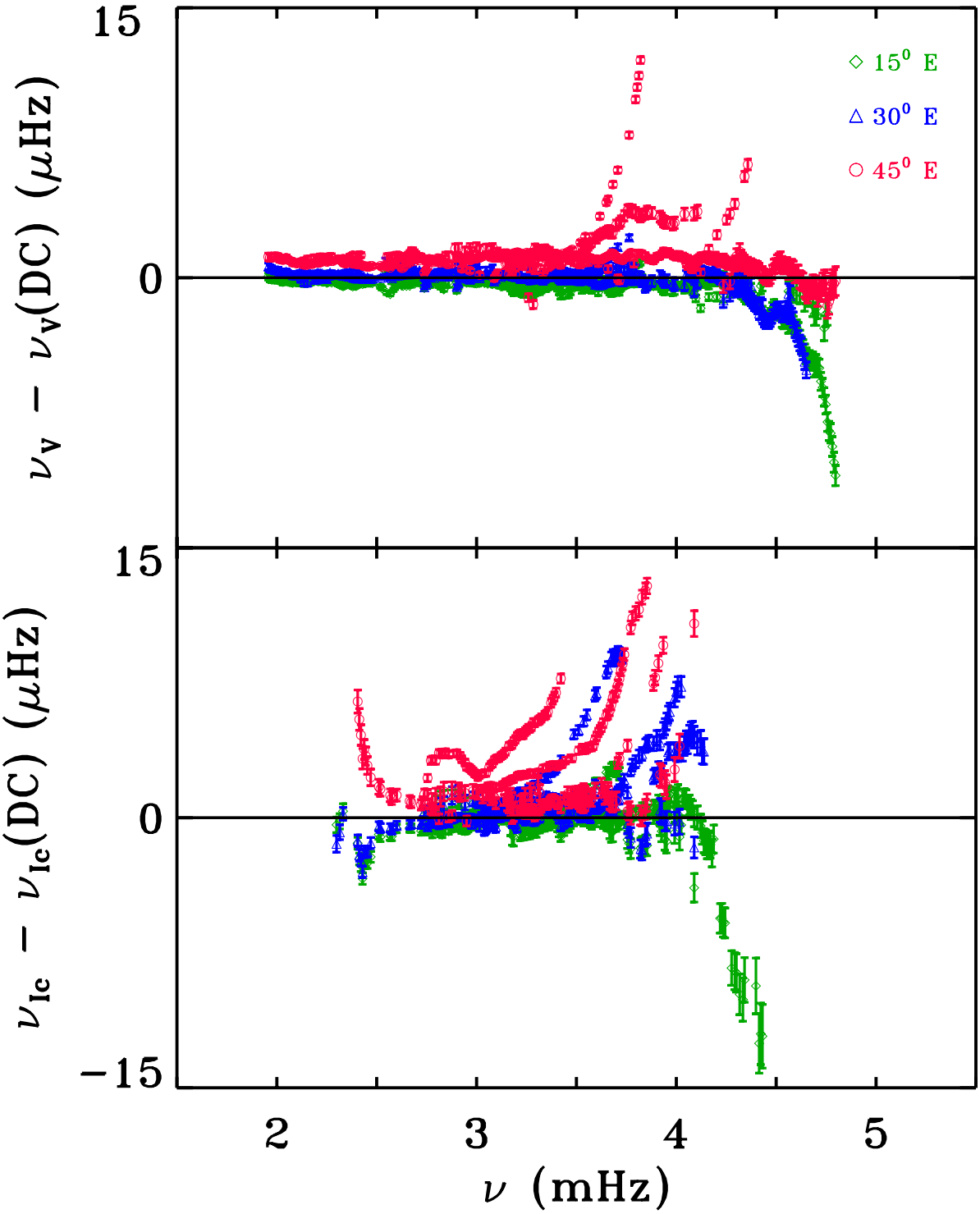

Fig. 9.— Frequency shifts between velocity (top panel) and continuum intensity (bottom panel) modes at three different longitudes with respect to disk center obtained from the fit using asymmetric profiles. The locations are marked in the top panel.